Exploring partial control of chaotic systems

Samuel Zambrano and Miguel A. F. Sanjuán
Departamento de Física, Universidad Rey Juan Carlos, Tulipán s/n, 28933 Móstoles, Madrid, Spain
(Received 30 July 2008; published 23 February 2009)

In this paper we make a thorough exploration of the technique of partial control of chaotic systems. This control technique allows one to keep the trajectories of a dynamical system close to a chaotic saddle even if the control applied is smaller than the effects of environmental noise in the system, provided that the chaotic saddle is due to the existence of a horseshoelike mapping in phase space. We state this here in a mathematically precise way using the Conley-Moser conditions, and we prove that they imply that our partial control strategy can be applied. We also give an upper bound of the control-noise ratio needed to achieve this goal, and we describe how this technique can be applied for large noise values. Finally, we study in detail the effect of imperfect targeting in our control technique. All these results are illustrated numerically with the paradigmatic Hénon map.

DOI: 10.1103/PhysRevE.79.026217 PACS number(s): 05.45.Gg

I. INTRODUCTION

In recent years, control of chaotic dynamical systems [1] has attracted growing attention due to the ubiquity of this kind of systems in nature and its potential applications in science and engineering [2]. A feature shared by most control techniques is that they attempt to obtain a desired behavior from a dynamical system by applying small and accurately chosen perturbations. To do this, it is often needed to use appropriately some of the properties of the dynamical system under consideration. A paradigmatic example of this approach is the seminal paper by Ott, Grebogi, and Yorke [3], where the properties of the chaotic attractor are used to stabilize the trajectories of the system onto a desired periodic orbit embedded within it.

But permanent chaos is just one among many dynamical phenomena that can be observed in nonlinear dynamical systems. Transient chaos [4] is also widespread. This phenomenon is due to the existence of a nonattractive chaotic set in phase space, the so-called chaotic saddle: Trajectories that start close to a chaotic saddle will behave chaotically for a while before settling into another (possibly periodic) attractor. For this reason, there are situations where it is preferable to keep the trajectories close to the chaotic saddle, so different techniques to achieve this goal have been proposed [5–11], referred to typically as the control of transient chaos.

Because the chaotic saddle is a zero-measure repelling set in phase space, in order to keep the trajectories nearby, it will be necessary to apply repeated corrections to the trajectories of the system considered, i.e., a control. But this is not the only difficulty that must be faced when trying to achieve this goal: Typically, most real systems are affected by the presence of environmental noise.

In most realistic situations, the control that can be applied on the system's trajectories is bounded. Thus, we must consider different scenarios. If the control that can be applied on the system's trajectories is larger than the amplitude of the noise, we might presumably easily find a control strategy to keep the trajectories close to the chaotic saddle. On the other hand, if the control that can be applied on the system is equal to the amplitude of the noise, the strategies cited above allow one to keep the trajectories close to the chaotic saddle. But there is another possibility: It might well happen that the control that can be applied on the system is smaller than the amplitude of the noise. In this situation, due to the intrinsic instability of the chaotic saddle and the effect of noise, the control of transient chaos might seem impossible to achieve.

However, in a recent paper [12] we sketched a technique that allows one to keep the trajectories close to the chaotic saddle even in this complicated scenario. As in other control techniques, our control technique makes use of the particular characteristics of the dynamics that give rise to this type of behavior. The technique that we proposed made use of the fact that typically chaotic saddles arise due to the existence of a horseshoe map [13] in phase space. The particular geometrical action of this map is known to imply the existence of transient chaos on the system considered. However, we showed that precisely this geometrical action also implied the existence of certain sets, the safe sets, that can be used to keep the trajectories close to the saddle even if the corrections applied are smaller than the amplitude of the noise. Those sets lie in the vicinity of the chaotic saddle, and they turn out to have a structure such that trajectories can be kept on them even if the control applied is smaller than the effect of noise, which is a major advantage when compared with other control schemes. Among the cited references, only Ref. [9] gives a strategy that achieves an analogous result, that can be applied to a family of one-dimensional maps.

Our control scheme, though, does not say where the trajectories will exactly go in the vicinity of the chaotic saddle, so we call our technique partial control of a chaotic system. It is important to note that partial control has potential applications in many different contexts in physics, due to the ubiquity of horseshoelike maps in nonlinear dynamical systems. Since the pioneering work of Smale [14], horseshoe maps have played an important role in understanding chaotic dynamics, and they are known to be present in the dynamical systems used to model different physical phenomena: A particle bouncing on an oscillating table [15], a driven laser [16], a family of nonlinear oscillators [17], an atom-field interaction [18], a bistable optical system [19], a Josephson junction [20], and in fluid advection [21], just to cite some examples.

The aim of this paper is to prove some of the results stated in Ref. [12], in order to make it clear that the technique described there can be applied to a wide class of dynamical systems with a chaotic saddle. On the other hand, we give some results that enlighten different aspects of our partial control technique, such as an upper bound of the control needed and the effect of imperfect targeting of the safe sets. Our ideas are illustrated with the paradigmatic Hénon map, that we also use to verify numerically the validity of our results.

The structure of this paper is the following: First, we will state in a mathematically precise way our problem in Sec. II, formulating the existence of a horseshoelike mapping on phase space in terms of the Conley-Moser conditions [22]. In Sec. III we prove that these quite general conditions imply necessarily the existence of safe sets, and thus our partial control technique can be applied. In Sec. IV we briefly describe our partial control technique and use it to give an upper bound of the control-noise ratio needed to keep trajectories bounded, and we show that it is always smaller than one. We discuss in Sec. V the effects of imperfect targeting, and finally in Sec. VI the main results of this paper are summarized.

II. PROBLEM STATEMENT

We start by stating our problem in a mathematically precise way. We consider here that the dynamics of the unperturbed system that we want to control is given by the two-dimensional map $\mathbf{p}_{n+1}=\mathbf{f}(\mathbf{p}_n)$. The main properties of the maps considered here will be given later, but they can be characterized by having a chaotic saddle on a square Q in phase space, in such a way that nearly all the trajectories (except a zero measure set) will escape from Q after a finite number of iterations. We can also consider that, as in most physical systems, this dynamical system is affected by environmental noise. The noise here can be modeled by adding a random perturbation $\mathbf{u}_n$ each iteration, such that $0<\|\mathbf{u}_n\| \leqslant u_0$. Thus, the dynamics of the system that we want to control can be modeled by the equation $\mathbf{p}_{n+1}=\mathbf{f}(\mathbf{p}_n)+\mathbf{u}_n$.

As we said, our aim is to keep the trajectories close to the chaotic saddle, and thus inside Q, by applying an accurately chosen and bounded control $\mathbf{r}_n$, that is, $0<\|\mathbf{r}_n\|\leqslant r_0$. We assume that this control can be applied upon each iteration on the system's trajectory, so the global dynamics of the system is given by the following equation:

$$\mathbf{q}_{n+1} = \mathbf{f}(\mathbf{p}_n) + \mathbf{u}_n,$$

$$\mathbf{p}_{n+1} = \mathbf{q}_{n+1} + \mathbf{r}_n(\mathbf{q}_{n+1}). \tag{1}$$

These equations simply mean that, considering the position $\mathbf{p}_n$, each iteration on the joint action of the map and the noise would make the trajectory lie on $\mathbf{q}_{n+1}$. However, for each iteration we apply a control that depends on $\mathbf{q}_{n+1}$, $\mathbf{r}_n(\mathbf{q}_{n+1})$, so that the next point of the trajectory $\mathbf{p}_{n+1}$ will be close to the chaotic saddle.

In Ref. [12] we mention that if we wanted to apply our partial control technique, the map $\mathbf{f}$ needed to be horseshoelike. This can be mathematically formulated by saying that the map $\mathbf{f}$ satisfies a slight modification of the Conley-Moser conditions as they can be found in Ref. [23]. In order to state these conditions, some definitions are needed. For simplicity, consider that the square Q is placed in the plane in such a way that the top and bottom sides are parallel to the x axes, and the left- and right-hand sides are parallel to the y axis. We consider that a horizontal curve is a curve going from the left-hand to the right-hand side of Q of the form $[x,g(x)]$. Analogously, a vertical curve is a curve $[h(y),y]$ going from top to bottom of the square Q. A horizontal strip is the set of points between two nonintersecting horizontal curves, and a vertical strip is the set of points lying between two nonintersecting vertical curves. The width of a horizontal strip H, noted $w(H)$, is the maximum distance between any two points of the bounding horizontal curves sharing the same x coordinate. Analogously, the width of a vertical strip V, noted $w(V)$, is the maximum distance between any two points of the bounding vertical curves sharing the same y coordinate.

Considering these definitions, the map $\mathbf{f}$ needs to satisfy the following conditions:

(C1) For a certain square Q in the plane, $\mathbf{f}(Q)\cap Q$ consists of at least two disjoint horizontal strips H_1 and H_2 that are separated from the upper and lower sides of Q by a distance $\Delta>0$, and $\mathbf{f}^{-1}(Q)\cap Q$ consists of at least two vertical strips V_1 and V_2. Moreover, $\mathbf{f}(V_i)=H_i$ homeomorphically and the horizontal (vertical) bounds of V_i are mapped into horizontal (vertical) bounds of H_i.

(C2) Given a horizontal strip H, then $\mathbf{f}(H)\cap H_i$ for $i=1,2$ is a horizontal strip satisfying

$$w[\mathbf{f}(H)\cap H_i] \leqslant \nu w(H) \quad \text{with } \nu \in (0,1).$$

For any vertical strip V, $\mathbf{f}^{-1}(V)\cap V_i$ for $i=1,2$ is also a vertical strip satisfying

$$w[\mathbf{f}^{-1}(V)\cap V_i)] \leqslant \nu w(V) \quad \text{with } \nu \in (0,1).$$

These conditions are illustrated in Fig. 1. As the reader will notice, they match with the intuitive notion of a horseshoelike mapping on Q, i.e., a mapping that stretches and folds the square on phase space back into itself.

From C1 and C2 two facts can be derived [23]: First, that there is a zero-measure set where the dynamics is chaotic, the chaotic saddle. Second, that all trajectories starting in Q, except a zero measure set, escape from it under a finite number of iterations. Thus, a map satisfying these conditions is a good example of dynamical system with a chaotic saddle. Furthermore, conditions similar to C1 and C2 can be derived for any map with transverse homoclinic points by the Smale-Birkhoff homoclinic theorem [15], so we can say that maps satisfying these conditions can be found in quite general situations. These are the dynamical systems that we want to control: We shall show now that these conditions also imply that trajectories can be kept inside Q, and thus can be partially controlled, even if $r_0<u_0$.

An example of a map satisfying these conditions is the well-known Hénon map $x_{n+1}=A-By_n-x_n^2$, $y_{n+1}=x_n$ with $A=6$, $B=0.4$. By adequately choosing a square Q in phase space, this map looks like a horseshoe map, as shown in Fig. 2. By verifying that this map satisfies C1 and C2, it can be

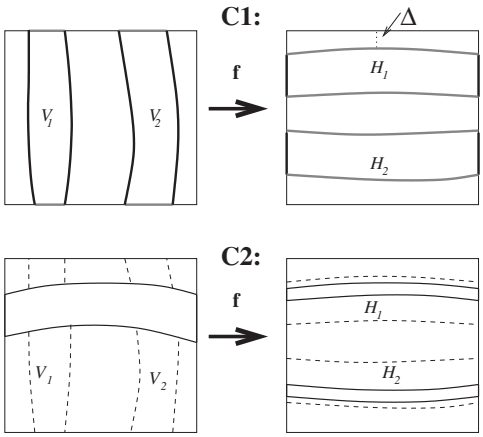

FIG. 1. A pictorial representation of the conditions C1 and C2. Condition C1 says that inside the square Q there are at least two vertical strips V_1 and V_2 that are mapped to two horizontal strips H_1 and H_2, in such a way that horizontal bounds of H_i (gray) are mapped into horizontal bounds (gray) of V_i, and the same applies to vertical bounds (black) of H_i and V_i. The minimum distance between the top or the bottom of Q and the strips H_1 and H_2 is noted Δ. Condition C2 says that if we apply the map $\mathbf{f}$ to a horizontal strip H and we look at the intersection of $\mathbf{f}(H)$ with H_1 and H_2, we will find two horizontal strips thinner than H. A similar phenomenon occurs when we apply $\mathbf{f}^{-1}$ to a vertical strip V and we look at the intersection of $\mathbf{f}^{-1}(V)$ with V_1 and V_2.

proved that there is a chaotic saddle inside Q [24]. On the other hand, it can be shown that nearly all the trajectories starting in Q, except a zero-measure set, diverge to infinity after a number of iterations. Thus, by applying our control technique to this system we will show that it is possible to keep trajectories close to the saddle, and thus bounded, even if the control applied is smaller than the amplitude of noise.

III. SAFE SETS

Now we are going to show that from the conditions C1 and C2 given in the preceding section, the existence of safe sets—the key element of our partial control strategy—can be inferred. In Ref. [12] we stated that if the map $\mathbf{f}$ acts like a horseshoe map, and if we call S^0 to the vertical curve lying

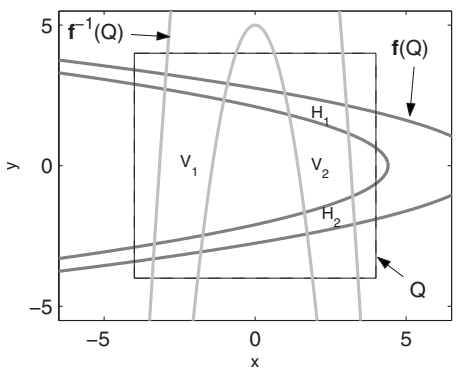

FIG. 2. The action of the Hénon map $x_{n+1}=6-0.4y_n-x_n^2$, $y_{n+1}=x_n$ in a square Q on the plane. This map satisfies conditions C1 and C2, so our technique can be applied.

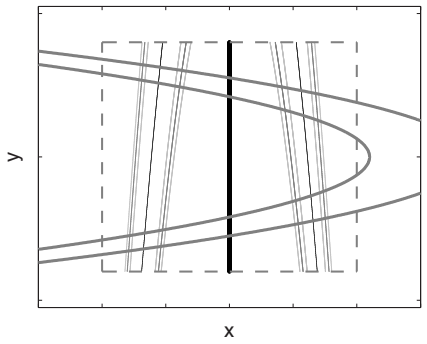

FIG. 3. The safe sets for the Hénon map S^0 (thick line), S^1 (black line), S^2 (gray line), and S^3 (light gray line). The square Q (−) and its image under the map (thick gray) are also plotted for the sake of clarity. Note that they fulfill properties (i)–(iii): The set S^k consists of 2^k vertical curves, each of them having two adjacent vertical curves of S^{k+1} closer to it than any other curve of S^k, and the distance with these adjacent curves decreases with k.

between the two vertical strips V_1 and V_2, the sets $\{S^j\}$ generated inductively as

$$S^k = \mathbf{f}^{-1}[S^{k-1} \cap (H_1 \cup H_2)], \tag{2}$$

are the safe sets and they fulfill the following properties (i)–(iii):

(i) S^k consists of 2^k vertical curves.

(ii) Any vertical curve of S^k has two adjacent vertical curves of S^{k+1} closer to it than any other curve of S^k.

(iii) The maximum distance between any of the 2^k curves of S^k and its two adjacent curves of S^{k+1}, denoted as $\delta^k_{\max}$, goes to zero as $k \to \infty$. The same applies to the minimum distance, denoted $\delta^{k-1}_{\min}$.

In order to illustrate clearly these properties, we have calculated the safe sets for the Hénon map, and they are shown in Fig. 3. They clearly satisfy conditions (i)–(iii), as expected. With this example in mind, we can prove now that for any map $\mathbf{f}$ satisfying the conditions C1 and C2 the safe sets calculated using Eq. (2) will also satisfy conditions (i)–(iii).

We start by proving condition (i). Hypothesis C1 implies that, given a vertical curve C, $\mathbf{f}^{-1}(C) \cap V_i$ is a vertical curve for $i=1,2$. Thus, if S^0 is a vertical curve that lies between V_1 and V_2, obviously S^1 consists of two disjoint vertical curves, one to its left and the other to its right. Considering that $\mathbf{f}^{-1}$ is a homeomorphism from H_i to V_i, and that the curves in S^1 are disjoint, $S^2=\mathbf{f}^{-1}(S^1) \cap (V_1 \cup V_2)$ consists of four disjoint vertical curves. Reasoning inductively, it is clear that the set S^k given by Eq. (2) consists of 2^k disjoint vertical curves, as we had for the Hénon map.

The proof of condition (ii) is analogous. Clearly, condition (ii) holds for $k=0$. Assume that (ii) holds for k. Then each curve in S^k has two adjacent curves in S^{k+1}. Thus, each of the 2^k vertical curves of S^k is inside a vertical strip bounded by those adjacent curves of S^{k+1}. If we apply the map $\mathbf{f}^{-1}$ to each of these strips and see its intersection with V_1 and V_2, by C2 we will have 2^{k+1} nonintersecting vertical strips. Each of them will be bounded by two curves, which by definition are curves of S^{k+2}. On the other hand, each strip

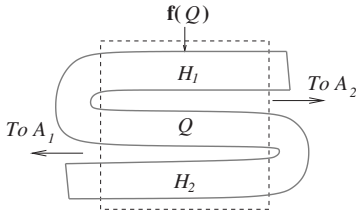

FIG. 4. The action of the map **f** on the square Q (dashed line). If we assume that points to the right of the right-hand side of Q settle after iterates into a periodic attractor A_1, and that points to the left of the left-hand side of Q settle after iterates into a periodic attractor A_2, it can be shown that this type of mapping implies the appearance of fractal boundaries between the basins of attractions of those attractors. But this type of geometrical action would also allow us to build safe sets that can keep trajectories inside Q in the presence of noise with $r_0 < u_0$.

will contain a curve that is a curve of S^{k+1} by definition. Thus, each curve of S^{k+1} has two adjacent curves of S^{k+2} closer to it than any other curve of S^{k+1}, due to the fact that the strips constructed as described above cannot intersect. Considering this, condition (ii) holds for $k+1$ and thus for all k, as claimed.

Finally, condition (iii) can be proved by observing that the maximum and the minimum distance between any curve of S^k and its two adjacent curves of S^{k+1} is bounded by the width of the 2^k strips that we described above, which clearly by hypotheses C2 decreases as ν^k with k.

It is important to notice, however, that these conditions imply the existence of safe sets for maps that do not necessarily stretch and fold the square in a Smale-horseshoelike way, as the Hénon map does. Condition C1 simply demands that $\mathbf{f}(Q) \cap Q$ and $\mathbf{f}^{-1}(Q) \cap Q$ consist of at least two horizontal and vertical strips, respectively, that are mapped among themselves in a suitable way. Thus, different maps can fulfill this condition. An example of this is the map that is sketched in Fig. 4. It can be shown [25] that if we consider a map **f** that stretches and folds the square Q as shown there, in such a way that points to the left and the right of Q under iterations settle into the distant periodic attractors A_1 and A_2, respectively, then fractal basin boundaries arise. However, this kind of mapping also satisfies conditions C1 and C2 (we have two strips H_1 and H_2 under which the map acts in the prescribed way), so safe sets can be found for this system and trajectories could be kept inside Q, and thus away from these attractors, forever with $r_0 < u_0$, as we will see below.

On the other hand, horseshoes usually appear in settings quite different to those discussed above. As we said in the preceding section, the Smale-Birkhoff homoclinic theorem [15] assures that close to a transverse homoclinic point, we can find a topological square for which the action of the considered map (or of a number of iterations of the considered map) is topologically equivalent to a horseshoe map. Moreover, it can be shown that in those situations it is possible to find a (topological) square in this situation for which the dynamical system considered acts on it in a way that is topologically equivalent to the action of a map acting on a square Q satisfying conditions C1 and C2. Considering this, in these general settings it is possible to find safe sets that are topologically equivalent to those described by properties (i)–(iii), so the set S^k is always "surrounded" by the set S^{k+1}. From the control strategy that we will describe below, it will be clear that this is the key property of those safe sets. Thus, the results provided in this paper show that our control technique can be applied in a wide variety of situations.

In this context, an important problem is how those topological horseshoes can be detected. To our knowledge, there is not a general approach to achieve this goal. Although this goal is far from the scope of the present work, we consider that there are two tools that can be used in order to detect those horseshoes. The first one would be to detect the periodic orbit with a transverse homoclinic point by detecting and computing its stable and unstable manifolds, something that can be done even experimentally [26]. Once this is done, it must be possible to find a suitable topological square enclosing it where the system will behave like a horseshoe map. Another possible approach would be to use a method to detect the chaotic saddle (for example, the one proposed in [27]) and to observe the action of the map on an adequate square enclosing it, which might allow us to observe a horseshoelike mapping.

Considering this, we have proved that the conditions C1 and C2 imply the existence of these advantageous safe sets. With these ideas we can describe now how our partial control technique uses them. We will give later an upper bound of the control-noise ratio needed for our partial control technique as a function of the noise amplitude u_0.

IV. PARTIAL CONTROL STRATEGY: CONTROL-NOISE RATIO

We consider first the case $u_0 \leqslant \Delta$, and we will treat the less aesthetically appealing case $u_0 \geqslant \Delta$ later. The strategy described in [12] was essentially the following: Given the value of the noise amplitude u_0, we must place the initial condition of the system $\mathbf{p_0}$ on a suitable safe set S^k such that $\delta_{\max}^{k-1} < u_0$ [which always exists no matter how small u_0 is by property (iii)]. After this, considering that S^k is the preimage of S^{k-1} in the square Q, $\mathbf{f}(\mathbf{p_0})$ will be on a curve of S^{k-1}, which has two adjacent curves of S^k, by (ii).

The deviation induced by noise can essentially have two effects, that are summarized in Fig. 5. First, it can make the perturbed trajectory $\mathbf{q}_1 = \mathbf{f}(\mathbf{p}_0) + \mathbf{u}_0'$ lie in the region between those two curves of S^k. Another possibility is that the perturbed trajectory will lie outside this region, in the point $\mathbf{q}_1 = \mathbf{f}(\mathbf{p}_0) + \mathbf{u}_0$. In the previous case, and by definition of $\delta_{\max}^{k-1}$, a correction $\mathbf{r_0}$ smaller or equal to $\delta_{\max}^{k-1}$ (and thus smaller than u_0) will put the point of the trajectory back on a curve of S^k. In the latter case, it is clear that a correction smaller than $u_0 - \delta_{\min}^{k-1}$ can place it back on a curve of S^k, as we can see in Fig. 5. Thus, using this strategy we can always find a $\mathbf{r}_0$ whose length is bounded $\|\mathbf{r}_0\| \leqslant r_0 < u_0$ in such a way that the next point of the trajectory $\mathbf{p}_1 = \mathbf{q}_1 + \mathbf{r}_0$ will lie again on S^k, and this can be repeated forever. This implies that using this strategy we can always find a positive constant r_0 such that even if $\|\mathbf{r}_n\| \leqslant r_0 < u_0$ the trajectory $\mathbf{p}_n$ lies always somewhere on S^k, and the system is partially controlled forever.

In the example described before, we should search for the point of S^k that is the closest to $\mathbf{q}_1$ and then compute $\mathbf{r}_0$, and

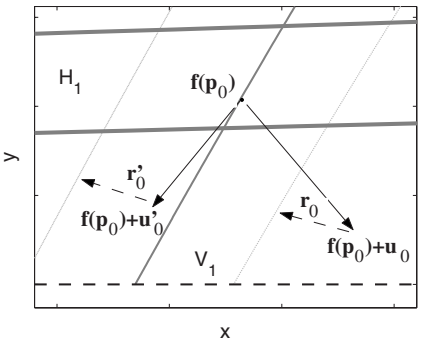

FIG. 5. A trajectory starting in $\mathbf{p_0}$ belonging to S^3 (light gray line) is mapped to $\mathbf{f}(\mathbf{p_0})$, that belongs to S^2 (gray line). The noise action can either deviate it to the region between the two adjacent curves belonging to S^3, as $\mathbf{u}_0'$, or take it outside this region, as $\mathbf{u_0}$. In any case, trajectories can be placed again on S^3 by applying a perturbation (either $\mathbf{r}_0'$ or $\mathbf{r_0}$) bounded by a r_0 such that $r_0 < u_0$, and this can be repeated forever.

repeat the same procedure for each iteration. In principle, we will have only a limited number of points of S^k stored, but if the number of such points is sufficiently big the technique described above can be applied properly.

This type of control might face some difficulties in practical situations, though. The presence of inaccuracies in the location of S^k or of imperfect targeting, i.e., of errors in the applied control $\mathbf{r}_n$, might be an obstacle for this type of control, although we will show in the next section that they do not have a dramatic effect if those inaccuracies are reasonably small. Another possible problem when applying this technique would be that we will need to apply the correction inmediatley upon each iteration, so that a given amount of time will be needed to locate the point on S^k that lies closest to $\mathbf{q}_n$. The search of such a point can be slow if we have a lot of points stored as belonging to S^k, something that on the other hand is necessary for a correct application of our control technique, as we said above. However, we know how the points of S^k are mapped into points of S^{k-1}. For example, in the description of the strategy above, provided the position of $\mathbf{p}_0$, we know beforehand that $\mathbf{q}_1$ will be close to a particular point of S^{k-1}, namely $\mathbf{f}(\mathbf{p}_0)$. Thus, using adequately this information can reduce the search time drastically.

As an example of application of our technique, we can apply it to the Hénon map. We consider the case in which the system is affected by noise with amplitude $u_0=0.25<\Delta \approx 0.7$. Numerical computations of the $\delta^k_{\max}$ show that the suitable safe set S^k for our control strategy is S^3. In Fig. 6(a), we can see the trajectory resulting from applying our partial control strategy in 1000 iterations. The points of the resulting trajectory lie always somewhere on S^3, and in Fig. 6(b) we can see that the amplitude of the control applied each iteration $\|\mathbf{r}_n\| \leqslant r_0 \approx 0.18$ is smaller than $u_0=0.25$. Thus, divergences from Q are avoided even if the correction applied for each iteration is smaller than the noise amplitude. It is important to note that in absence of control and of noise, a trajectory starting on S^3 would typically escape from the square Q after four iterations, and then diverge.

An important issue here is to consider which would be the control-noise ratio r_0/u_0 allowing to partially control the system considered for different values of $u_0<\Delta$. Considering the strategy described above, that $\delta^k_{\min} < \delta^{k-1}_{\min}$ and that $\delta^k_{\max} < \delta^{k-1}_{\max}$, it is straightforward to show that the control-noise ratios needed for each value of $u_0 \leqslant \Delta$ are bounded by the following expressions:

$$\frac{r_0}{u_0} \leqslant \frac{\delta^k_{\max}}{u_0} \quad \text{if } u_0 \in [\delta^{k-1}_{\max} + \delta^k_{\min}, \delta^{k-1}_{\max} + \delta^{k-1}_{\min}],$$

$$\frac{r_0}{u_0} \leqslant \frac{u_0 - \delta^{k-1}_{\min}}{u_0} \quad \text{if } u_0 \in [\delta^{k-1}_{\max} + \delta^{k-1}_{\min}, \delta^{k-2}_{\max} + \delta^{k-1}_{\min}].$$

Obviously these expressions give upper bounds of the ratios that are smaller than 1, and they depend on the value of the noise u_0 considered. These expression also give us an indication of the safe set S^k that allows one to minimize the ratio r_0/u_0, given the value of u_0. The lower bound of these ratios is $r_0/u_0=1/2$, which means that in some cases the system considered can be partially controlled with a control that is 50% of the noise. This fact, though, will depend on the value of u_0 and on the size of the δ's, whose value depend on the map $\mathbf{f}$.

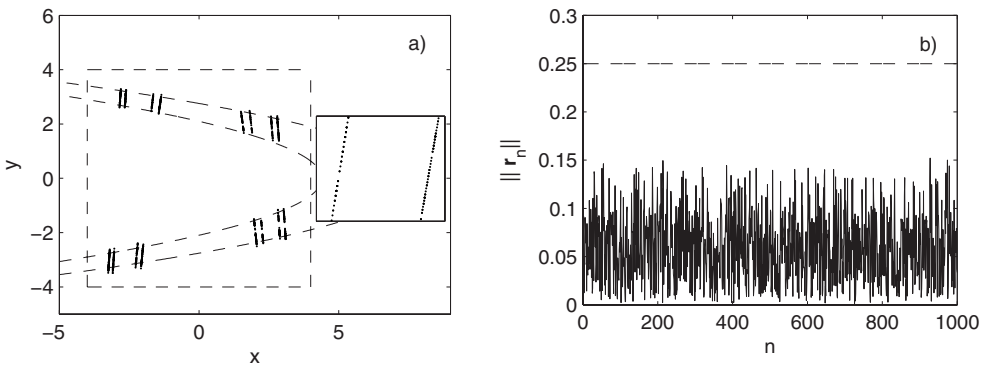

FIG. 6. Example of application of our strategy to the Hénon map for $u_0=0.25$. (a) A plot of 1000 points or the orbit, that lie on S^3, the suitable safe set for this value of noise. The square Q and its image under the map (dashed line) are also plotted for the sake of clarity. The inset plot shows a zoom of the square, showing that the points of the trajectory always fall on the curves of S^3. (b) The value of the control applied for each iteration is to keep the trajectories on S^3 and thus on Q. Note that it is always smaller than $u_0=0.25$ (marked with a dashed line), as expected.

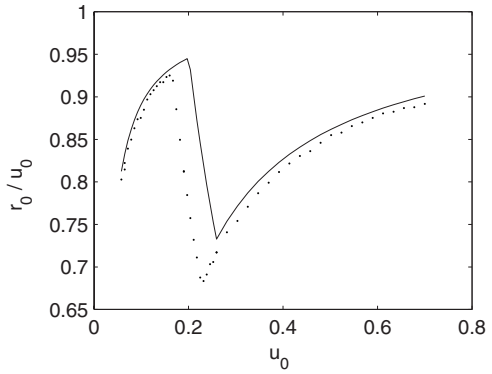

FIG. 7. Control-noise ratio needed to partially control the Hénon map, computed numerically taking 1000 trajectories of 1000 iterations (dots). We also plot (solid) the upper bounds for this ratio given by the expression derived in the text. In order to use those expressions, numerical estimates of the values of $\delta^k_{\max}$ and $\delta^k_{\min}$ are needed.

In order to verify the validity of these bounds, we have computed them numerically for the Hénon map by taking a series of 1000 time steps for different values of u_0, and we have numerically estimated the ratio of r_0/u_0 needed to partially control the system. The result of our calculation can be seen in Fig. 7, where the ratio is plotted against u_0. We can see in that figure that there is a good agreement between the computed values and the upper bounds given above, that were computed using numerical estimations of the $\delta^k_{\max}$ and $\delta^k_{\min}$ involved.

Finally, we can show how our control strategy can be applied even if the noise values are large, i.e., if $u_0 > \Delta$. For these noise values the control strategy that we apply is essentially the same: We just need to put the initial condition on a suitable safe set S^k, from which it will be mapped to a point in S^{k-1}. Condition C1 implies that any point on a safe set will be mapped inside a horizontal strip, either H_1 or H_2, and that it will be at most Δ away from the top or the bottom sides of the square Q. Thus, when $u_0 > \Delta$, it is possible to find that the joint action of the noise and the map can take the trajectory out of the square, as shown in Fig. 8. Considering the situation shown in this figure, it is easy to see that it is still possible to keep the trajectories bounded for a given value of $u_0 > \Delta$. What we must do is to place the initial condition on a safe set S^k such that u_0 is larger than $\max\{u_0 - \Delta + \delta^{k-1}_{\max}, \delta^{k-1}_{\max}\}$, which is always possible provided that k is sufficiently small. In that case, we can see that it is possible to keep trajectories bounded forever with $r_0 < u_0$. The necessary r_0 value to achieve this goal is

$$r_0 = \max\{u_0 - \Delta + \delta^{k-1}_{\max}, \delta^{k-1}_{\max}, u_0 - \delta^{k-1}_{\min}\} < u_0.$$

This possibility, together with the possibilities discussed in the $u_0 \leqslant \Delta$ case, imply that we can keep trajectories bounded forever with $r_0 < u_0$ for all values of $u_0 > 0$.

V. EFFECTS OF IMPERFECT TARGETING

As in any other control scheme involving targeting of certain points in phase space, an important issue that should be considered when aiming for potential practical applications is which can be the possible effects of having imperfect targeting. This can be modeled by considering that, instead of applying the necessary correction $\mathbf{r}_n$ for each iteration, we apply $\mathbf{r}_n + \Delta\mathbf{r}_n$, where $\|\Delta\mathbf{r}_n\| < \Delta r_0$ is what we call "control noise." This is a random error out of our control that is due to this imperfect targeting. However, it is important to note that this situation is equivalent to considering that we do not know the exact position of the safe sets S^k, but instead there is an inaccuracy smaller or equal than Δr_0 on its position. Thus, this Δr_0 can be an effect of the imperfect targeting, to uncertainties in the position of the safe sets or to these two effects together.

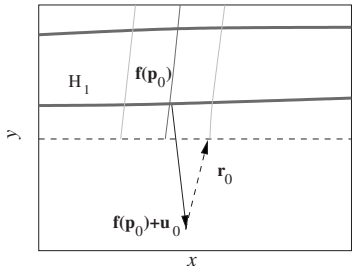

FIG. 8. A possible situation arising when $u_0 > \Delta$. A trajectory starting in $\mathbf{p_0}$ belonging to S^3 (light gray line) is mapped to $\mathbf{f}(\mathbf{p}_0)$, that belongs to S^2 (gray line), a point that is inside the horizontal strip H_1 (bounds in thick gray lines). If $u_0 > \Delta$ the point $\mathbf{f}(\mathbf{p}_0) + \mathbf{u}_0$ can lie out of Q, whose lower bound is also represented here (dashed). But if we have chosen adequately the set S^k, we can see here that with a control $\mathbf{r}_0$ bounded by a r_0 such that $r_0 < u_0$, the trajectory can be lead to S^k, and this can be repeated forever.

However, as we sketched in Ref. [12], it is not difficult to show that in this situation it is still possible to keep trajectories bounded even when the control is smaller than the noise if Δr_0 is sufficiently small. This can be seen as follows. Assume that we are trying to partially control the trajectory for a given u_0, and that this can be achieved when the targeting is perfect (which implies that $\Delta r_0 = 0$) for certain value $r_0 < u_0$. For simplicity, we can assume that $\mathbf{p}_n$ is a point that can be at most Δr_0 away from the suitable safe set S^k for this noise value. Considering that for $\Delta r_0 = 0$ the point $\mathbf{f}(\mathbf{p}_n) + \mathbf{u}_n$ will be at most u_0 away from a point in S^{k-1}, it is easy to see that for $\Delta r_0 \neq 0$, the point $\mathbf{q}_{n+1} = \mathbf{f}(\mathbf{p}_n) + \mathbf{u}_n$ will be further from S^{k-1}, but at most $u_0 + C\Delta r_0$ away from it. The value of the constant $C > 1$ depends on how expansive the map $\mathbf{f}$ is, but it can always be found for small Δr_0 values, as long as conditions C1 and C2 assure that the map $\mathbf{f}$ is well behaved.

As we mentioned before, in the case of perfect targeting a correction r_0 is enough to put the trajectory back on the safe set. Now that the deviation of the trajectory is larger (due to the joint action of noise $\mathbf{u}_n$ and to the fact that the trajectory did not lie exactly in the suitable safe set) we need to apply now a larger correction $\mathbf{r}'_n$. However, using the same idea that is shown in Fig. 5, we can notice that a correction such that $\|\mathbf{r}'_n\| \leqslant r'_0 = r_0 + C\Delta r_0$ would be enough to put $\mathbf{p}_{n+1} = \mathbf{q}_n + \mathbf{r}'_n$ at most Δr_0 away from the suitable safe set, and this strategy can be repeated forever. In this case, the necessary control and/or noise ratio to keep trajectories partially controlled is $r'_0/u_0 = (r_0 + C\Delta r_0)/u_0$, that is smaller than one if Δr_0 is sufficiently small, as we claimed.

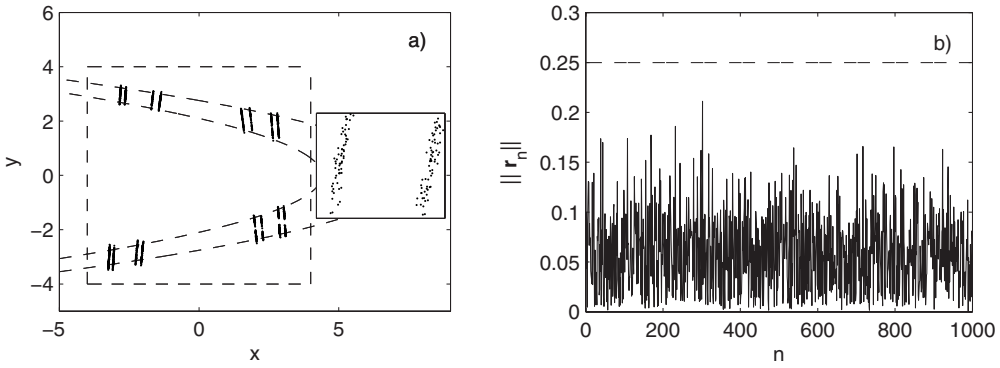

FIG. 9. Example of application of our strategy to the Hénon map for $u_0=0.25$, with a control noise such that $\Delta r_0 \approx 0.1 r_0$. (a) A plot of 1000 points or the orbit, that lie on S^3, the suitable safe set for this value of noise. The square Q and its image under the map (dashed line) are also plotted for the sake of clarity. The inset plot is a zoom of the square showing that now the points do not fall exactly on the safe set S^3, due to the presence of control noise. (b) The value of the control applied to each iteration to keep the trajectories on S^3 and thus on Q. Note that it is always smaller than $u_0=0.25$ (marked with a dashed line), as expected, in spite of the presence of control noise.

We have checked this result for different values of Δr_0 using the numerical example of the Hénon map with $u_0=0.25$, as we did previously. In Fig. 9 we can see a plot of a controlled trajectory and the applied correction $\|\mathbf{r}_n\|$ needed for each iteration to partially control the system in the presence of imperfect targeting, when $\Delta r_0=0.1 r_0$. We can see in Fig. 9(a) plot of a controlled trajectory. The inset plot in that figure reveals that the trajectory lies always close to the suitable safe set S^3 but never exactly on it, due to the imperfect targeting. However, as we can see in Fig. 9(b), even in this situation the control applied is smaller than u_0. It is also clear, though, that the values of the control needed to keep the trajectories bounded using our strategy in this situation are larger than in the $\Delta r_0=0$ case [that are shown in Fig. 6(b)]. Thus, in our opinion this technique is quite robust to imperfect targeting.

VI. CONCLUSIONS

In this paper we have made a deep exploration of the partial control technique, a control strategy that allows one to keep the trajectories of a dynamical system close to a chaotic saddle even if the control applied is smaller than the noise amplitude. First, we have proved rigorously some results from which it can be inferred that our technique can be applied in quite general settings. After this, we have given results concerning this technique. We have derived upper bounds for the control-noise ratio that allow to partially control the considered system, that are always smaller than one. We have shown that our control strategy can also be used for large noise values. Finally, we have shown that those ratios can be kept smaller than 1 even if there are inaccuracies in the control signal, i.e., imperfect targeting, or uncertainties in the position of the safe sets. Our results have been illustrated and tested numerically with the paradigmatic Hénon map.

ACKNOWLEDGMENTS

This work was supported by the Spanish Ministry of Education and Science under Contract No. FIS2006-08525 and by Universidad Rey Juan Carlos and Comunidad de Madrid under Contract No. URJC-CM-2007-CET-1601.

[1] T. Shinbrot, C. Grebogi, E. Ott, and J. Yorke, Nature (London) **363**, 411 (1993).
[2] G. Chen and X. Yu, *Chaos Control: Theory and Applications (Lecture Notes in Control and Information Sciences)* (Springer-Verlag, Berlin, 2003).
[3] E. Ott, C. Grebogi, and J. A. Yorke, Phys. Rev. Lett. **64**, 1196 (1990).
[4] T. Tél, in *Directions in Chaos*, edited by Bai-lin Hao (World Scientific, Singapore, 1990).
[5] V. In, M. L. Spano, and M. Ding, Phys. Rev. Lett. **80**, 700 (1998).
[6] W. Yang, M. Ding, A. J. Mandell, and E. Ott, Phys. Rev. E **51**, 102 (1995).
[7] T. Tél, J. Phys. A **24**, L1359 (1991).
[8] M. Dhamala and Y. C. Lai, Phys. Rev. E **59**, 1646 (1999).
[9] J. Aguirre, F. d'Ovidio, and M. A. F. Sanjuán, Phys. Rev. E **69**, 016203 (2004).
[10] I. B. Schwartz and I. Triandaf, Phys. Rev. Lett. **77**, 4740 (1996).
[11] T. Kapitaniak and J. Brindley, Phys. Lett. A **241**, 41 (1998).
[12] S. Zambrano, M. A. F. Sanjuán, and J. A. Yorke, Phys. Rev. E **77**, 055201(R) (2008).
[13] K. T. Alligood, T. D. Sauer, and J. A. Yorke, *Chaos, An Introduction to Dynamical Systems* (Springer-Verlag, New York, 1996).
[14] S. Smale, Bull. Am. Math. Soc. **73**, 747 (1967).
[15] J. Guckenheimer and P. Holmes, *Nonlinear Oscillations, Dynamical Systems, and Bifurcations of Vector Fields* (Springer-Verlag, New York, 1983).
[16] I. B. Schwartz, Phys. Rev. Lett. **60**, 1359 (1988).

[17] F. C. Moon and G. X. Li, Phys. Rev. Lett. **55**, 1439 (1985).
[18] A. Nath and D. S. Ray, Phys. Rev. A **36**, 431 (1987).
[19] M. Taki, Phys. Rev. E **56**, 6033 (1997).
[20] M. Bartuccelli, P. L. Christiansen, N. F. Pedersen, and M. P. Soerensen, Phys. Rev. B **33**, 4686 (1986).
[21] M. A. F. Sanjuán, J. Kennedy, C. Grebogi, and J. A. Yorke, Chaos **7**, 125 (1997).
[22] J. Moser, *Stable and Random Motions in Dynamical Systems* (Princeton University Press, Princeton, NJ, 1973).
[23] S. Wiggins, *Introduction to Applied Nonlinear Dynamical Systems and Chaos* (Springer-Verlag, New York, 1990).
[24] R. Devaney and Z. Nitecki, Commun. Math. Phys. **67**, 137 (1979).
[25] S. W. McDonald, C. Grebogi, E. Ott, and J. A. Yorke, Physica D **17**, 125 (1985).
[26] I. Triandaf, E. M. Bollt, and I. B. Schwartz, Phys. Rev. E **67**, 037201 (2003).
[27] M. Dhamala, Y. C. Lai, and E. J. Kostelich, Phys. Rev. E **64**, 056207 (2001).